THE JOURNAL OF CHEMICAL PHYSICS **133**, 194306 (2010)

Experimental measurement of the van der Waals binding energy of $X-O_2$ clusters $(X=Xe, CH_3I, C_3H_6, C_6H_{12})$

Konstantin V. Vidma,[1,2,3] Georgii A. Bogdanchikov,[1,2,4] Alexey V. Baklanov,[1,2]
Dmitri A. Chestakov,[3] and David H. Parker[3,a)]
[1]*Institute of Chemical Kinetics and Combustion, Institutskaya Str. 3, Novosibirsk 630090, Russia*
[2]*Novosibirsk State University, Pirogova Str. 2, Novosibirsk 630090, Russia*
[3]*Institute for Molecules and Materials, Radboud University Nijmegen, Heijendaalseweg 135, 6525 ED Nijmegen, The Netherlands*
[4]*Institute of Computational Mathematics and Mathematical Geophysics (Computing Center), Lavrentjeva Ave. 6, Novosibirsk 630090, Russia*

(Received 13 July 2010; accepted 29 September 2010; published online 19 November 2010)

Van der Waals binding energies for the $X-O_2$ complexes $(X=Xe, CH_3I, C_3H_6, C_6H_{12})$ are determined by analysis of experimental velocity map imaging data for $O(^3P_2)$ atoms arising from UV-photodissociation of the complex [A. V. Baklanov *et al.*, J. Chem. Phys. **126**, 124316 (2007)]. Several dissociation pathways have been observed, we focus on the channel corresponding to prompt dissociation of $X-O_2$ into $X+2O(^3P)$ fragments, which is present for complexes of O_2 with all partners X. Our method is based on analysis of the kinetic energy of all three photofragments, where the O atom kinetic energy was directly measured in the experiment and the kinetic energy of the X partner was calculated using momentum conservation, along with the measured angular anisotropy for O atom recoil. We exploit the fact that the clusters are all T-shaped or nearly T-shaped, which we also confirm by *ab initio* calculations, along with knowledge of the transition dipole governing radiative absorption by the complex. The effect of partitioning the kinetic energy between translation along the $X-O_2$ and O—O coordinates on the angular anisotropy of the O atom recoil direction is discussed. Van der Waals binding energies of $110 \pm 20\ cm^{-1}$, $280 \pm 20\ cm^{-1}$, $135 \pm 30\ cm^{-1}$, and $585 \pm 20\ cm^{-1}$ are determined for Xe—O_2, CH_3I—O_2, C_3H_6—O_2, and C_6H_{12}—O_2 clusters, respectively. © *2010 American Institute of Physics*. [doi:10.1063/1.3503973]

I. INTRODUCTION

Van der Waals dimers have been extensively studied both experimentally and theoretically during the past several decades.[1–3] The main motivation in studies of weakly bound clusters is based on the fact that they are systems of intermediate complexity between individual molecules and the condensed phase. Investigation of small clusters with a well-known mutual configuration of the moieties and their interaction energies is a first step in understanding the influence of a weakly bound environment on various phenomena in the liquid phase, solid state, and interfaces.

The determination of the structure and binding energy of van der Waals clusters is of primary importance. These are parameters that can be directly compared with the results of quantum-chemical calculations as a test of the ability of theory to reproduce the characteristics of non-bonding interactions in such complexes, which are still not well understood.[4] Several methods for the experimental measurement of van der Waals cluster binding energies are currently in use,[1–3] especially mass analyzed threshold ionization (see, for example, Refs. 5–9), appearance threshold measurements,[10–12] or molecular beam scattering.[13,14]

In the present paper, we describe and apply a new method for experimental measurement of the bond energy in van der Waals clusters inspired by the results of our recent experiments on the photodissociation of $X-O_2$ clusters.[15] In that study, we detected the speed and angular distribution of O atoms arising from $X-O_2$ photodissociation at wavelengths around 226 nm by means of the velocity map imaging technique. For all $X-O_2$ clusters studied, strong enhancement in the O atom photoproduction cross-section was observed in comparison with the extremely weak photodissociation cross-section of an individual O_2 molecule. The enhanced signal revealed several channels for O atom formation where the main contribution arises from the channel $X-O_2+h\nu \rightarrow X+2O(^3P_j)$, and corresponds to excitation of the complex to a covalent state with excitation localized on the O_2 unit. This channel, denoted as channel 1 in Ref. 15, was observed for all $X-O_2$ clusters, and has a well pronounced negative anisotropy of O atom recoil (ejection perpendicular to the laser polarization direction). This signal was interpreted to be due to photodissociation of an $X-O_2$ complex with a T-shaped structure and a transition dipole moment direction perpendicular to the O—O axis. Directionality of the transition dipole moment was interpreted to arise from the admixture of an $X-O_2$ charge transfer state with the $^3\Delta_u$ excited covalent state of oxygen. Combined, this provides the preferentially negative anisotropy of O atoms recoil directions. However, the anisotropy parameter

---

[a)] Author to whom correspondence should be addressed. Electronic mail: parker@science.ru.nl.

value observed in Ref. 15 varies for different complexes. It is thus necessary to describe the angular anisotropy of O atoms recoil directions more quantitatively.

In the present paper, we show that the kinetic energy and angular distribution of fragment O atoms are determined in part by the $X-O_2$ van der Waals binding energy and that information on this energy can be extracted from the experimental velocity map imaging data. The value for binding energy can be also estimated on the basis of calculated structures. The use of these calculations and additional assumptions on the potential energy surface (PES) in the excited state of complex, including non-T-shaped complexes, will be illustrated for the propylene $C_3H_6—O_2$ complex.

Ab initio calculations have been performed in order to determine the geometry of $Xe—O_2$, $C_3H_6—O_2$, $CH_3I—O_2$, and $C_6H_{12}—O_2$ clusters. For $Xe—O_2$ clusters, experimental data on the $Xe—O_2$ potential reported by Aquilanti *et al.*[13] were also utilized.

II. DETAILS OF *AB INITIO* CALCULATIONS

Ab initio calculations of the geometry and binding energy of the $X-O_2$ complexes ($X=Xe, CH_3I, C_3H_6, C_6H_{12}$) have been carried out. As a first step, the geometry of individual X and O_2 molecules has been optimized and vibrational energies have been calculated. The geometries of the complex partners have been then used to reveal the most stable configurations of the complex. These configurations were then fully optimized within the basic approach specific for each complex. Two routines have been used then to calculate the binding energy. In approach 1 the geometry of minimum energy $E(XO_2)$ found with optimization was then used to calculate the zero point energy (ZPE) for $X-O_2$. In this variant the energy of optimized geometry has been corrected by taking into account the basis set superposition error (BSSE) by the counterpoise method.[16] The corrected energy $E_{BSSE}[XO_2]$ has been used in calculating the binding energy $E_{bind}=\Delta E+BSSE+\chi\cdot\Delta ZPE$, where $\Delta E=E(XO_2)-E(X)-E(O_2)$, $\Delta ZPE=ZPE(XO_2)-ZPE(X)-ZPE(O_2)$ and χ is the scaling factor fitting the calculated vibrational energies with the experimental ones for the free X and O_2 molecules. In approach 2, the calculation of BSSE has been involved in the optimization routine. In this variant the binding energy $E_{bind,BSSE}$ has been calculated via the equation $E_{bind,BSSE}=\Delta E_{BSSE}+\chi\cdot\Delta ZPE_{BSSE}$, where $\Delta E_{BSSE}=E_{BSSE}[XO_2]-E[X]-E[O_2]$ and $\Delta ZPE_{BSSE}=ZPE_{BSSE}[XO_2]-ZPE[X]-ZPE[O_2]$. Here the vibrational energies and so the ZPE of complex have been calculated by involvement of the BSSE contribution in the energy of complex. The approaches used for calculation of the geometry and energy of $Xe—O_2$, $CH_3I—O_2$, $C_6H_{12}—O_2$, and $C_3H_6—O_2$ differ due to the differences in complexity of these systems.

For the methyl iodide complex with oxygen, $CH_3I—O_2$, the MP2 approach[15] has been applied where an expanded basis set with the addition of polarization and diffuse functions has been used. For carbon, hydrogen, and oxygen atoms the aug-cc-pVTZ basis functions suggested by Dunning[17] have been utilized. For iodine atoms SDB-aug-cc-pVTZ basis functions elaborated by Martin and Sunderman[18] have been applied. These last functions in conjunction with a relativistic core polarization potential RECP suggested by Bergner, Dolg *et al.*[19] have been taken from the online version.[20]

For the complex $Xe—O_2$, the CCSD(T)//CCSD(T) approach has been used as a basic one. The aug-cc-pVTZ-PP (Ref. 21) for Xe and aug-cc-pVTZ basis set for O atom have been used in these calculations. For the complexes of cyclohexane $C_6H_{12}—O_2$ and propylene $C_3H_6—O_2$ the approaches MP2/6-31++G(d,p) and MP2/6-311++G(2d,2p), respectively, have been applied. All calculations have been carried out using the GAUSSIAN 03 package.[22]

III. EXPERIMENT

All experimental details are described in Ref. 15. Here we briefly mention the details that are important for the analysis presented in the current paper.

Clusters were prepared in the supersonic expansion of the gas mixture consisting of X (1%–2%) and O_2 (5%) seeded in buffer gas (mainly argon but in some experiments helium was also used).

The pulsed molecular beam was skimmed and then irradiated by pulsed radiation at the wavelength 225.655 nm (in vacuum) ($h\nu=44\,315.5\ \mathrm{cm}^{-1}$) that provided both the photoexcitation of clusters $X-O_2$ and selective ionization of nascent $O(^3P_2)$ atoms through a (2+1) resonance-enhanced multiphoton ionization (REMPI) process via the intermediate $(2s^22p^3(^4S°)3p)$ state.[23] The resulting O^+ photoions were detected by the velocity map imaging technique[24] and its recent "slicing" modification.[25] All results relevant to this particular study were obtained with the use of slicing method.[25] Slight detuning of the laser wavelength from the resonance value lead to complete disappearance of the O^+ ions signal, ensuring that all O^+ ions observed in the experiments are due to the resonant ionization of exclusively $O(^3P_2)$ atoms.

For kinetic energy calibration we use the ring in the image corresponding to $O(^3P_2)$ atoms arising from one-photon dissociation of individual molecules O_2 at the same wavelength

$$O_2+h\nu\rightarrow O(^3P_2)+O(^3P_j). \quad (1)$$

This ring is a superposition of three unresolved rings corresponding to the dissociation limits: $O(^3P_2)+O(^3P_2)$, $O(^3P_2)+O(^3P_1)$, and $O(^3P_2)+O(^3P_0)$. The dissociation to each limit produces two oxygen atoms with 1523.5, 1444.3, and 1410.0 cm^{-1} kinetic energy, respectively. Formation values for each of the channels are calculated using the expression $(h\nu-D_0(O_2)-E_{int}(^3P_J))/2$, where $h\nu=44\,315.5\ \mathrm{cm}^{-1}$ is the photon energy, $D_0(O_2)=41\,268.6\pm1.1\ \mathrm{cm}^{-1}$ (Ref. 26) is the dissociation energy of O_2, and $E_{int}(^3P_J)$ is the internal energy of $O(^3P_J)$ atoms. We used the values $E_{int}(^3P_2)=0$, $E_{int}(^3P_1)=158.265\ \mathrm{cm}^{-1}$, and $E_{int}(^3P_0)=226.977\ \mathrm{cm}^{-1}$.[23] The distribution of oxygen atoms over the fine structure states (^3P_j) arising in the photodissociation of O_2 at 226 nm was measured by Tonokura *et al.*[27] They found the branching ratio to be of 0.66, 0.27, and 0.07 for the states $^3P_0$, $^3P_1$, and $^3P_2$, respectively. With this branching ratio for O^3P_J atom partner

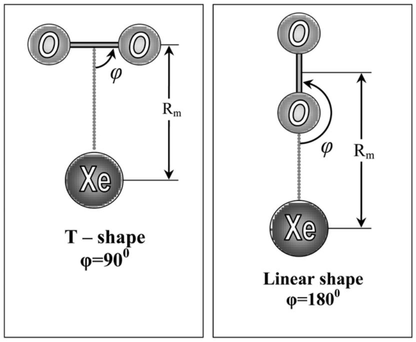

T-shape					
R_m, Å			E_{bind}, cm^{-1}		
Approach1	Approach2	Exp. [12]	Approach1	Approach2	Exp. [12]
3.81	4.00	3.87±0.08	61	86	144±7
L-shape					
4.28	4.52	4.30±0.09	28	74	104±5

FIG. 1. Geometry and binding energy of two stable configurations of the $Xe—O_2$ van der Waals complex. The inserted table contains the results of *ab initio* calculations carried out in the present work, as well as experimental data by Aquilanti *et al.* (Ref. 13) Calculation approaches 1 and 2 are described in Sec. II.

of detected $O(^3P_2)$, we obtain the average kinetic energy of $O(^3P_j)$ atoms for calibration

$$T_0 = (h\nu - D_0(O_2)) - \langle E_{int}(^3P_J)\rangle_0/2 = 1494.17 \ \ cm^{-1}. \quad (2)$$

For the $Xe—O_2$ system, an image due to photodissociation of free O_2 with the same O_2 percentage in Ar, but without Xe in the expansion mixture was subtracted before analysis of the cluster image. For the other three complexes, this subtraction was not necessary because the relative contribution due to photodissociation of free O_2 was negligible, as discussed in detail in Ref. 15.

For $CH_3I—O_2$ clusters, a series of test experiments with varied concentrations of CH_3I and O_2 molecules were performed in order to make sure that the observed signal originates from 1:1 clusters, and not from larger ones. For the other X partners, we assumed the probability of formation of clusters larger than 1:1 to be less than that for CH_3I, and therefore we assumed that for all partners X, the dominant clusters that produced in the expansion are 1:1 $X–O_2$ clusters. In some experiments we used He instead of Ar as the buffer gas in order to make sure that possible formation of clusters with Ar does not affect the results. More details of experiment can be found in the experimental section of Ref. 15.

IV. RESULTS OF *AB INITIO* CALCULATIONS

A. $Xe—O_2$

The results of calculations of the geometry and binding energy for the xenon-oxygen complex are presented on Fig. 1. Two stable isomers of the complex are found, corresponding to the triangular T-shaped and linear L-shaped forms. The same conclusions have been obtained earlier by Aquilanti *et al.* who studied the potential energy surface of the $Xe—O_2$ pair using scattering experiments.[12] The calculated geometry is found to be in a very good agreement with the experimentally established one. The calculated binding energy values are lower than the experimental ones but also indicate the predominance of T-shaped structure over the L-shaped one. The comparison with experimental binding energy also indicates the higher adequacy of approach 2, where the BSSE contribution is involved in the procedure of energy optimization.

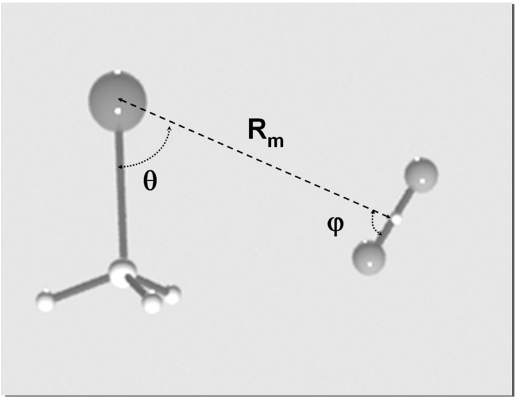

Approach1				Approach2			
θ	φ	R_m, Å	E_{bind}, cm^{-1}	θ	φ	R_m, Å	E_{bind}, cm^{-1}
67.2	77.6	3.91	187	68.6	76.7	3.96	203
179.7	89.3	3.57	164	179.8	89.8	3.67	174
285.5	102.6	3.92	167	284	103	3.97	185

FIG. 2. Calculated structure and binding energy for the isomers of the $CH_3I—O_2$ van der Waals complex. Three most stable types of isomers are found with geometry parameters shown in the table inset. All forms have C_S symmetry and a degeneracy factor of 3 corresponding to rotation of the O_2 subunit around the C_3 axis of the CH_3I subunit by 120°. The line connecting the center of the I atom and the center of mass of the O_2 subunit is almost perpendicular to the O—O bond in all of the isomers. Two used approaches of calculations approaches 1 and 2 are described in Sec. II.

B. $CH_3I—O_2$

The results of calculations of the geometry and binding energy for the complex of methyl iodide with oxygen $CH_3I—O_2$ are presented on Fig. 2. Three most stable configurations have been revealed. One configuration of I atom relative to the O—O axis is T-shaped and two others are close to the T-shaped one.

C. $C_6H_{12}—O_2$

The most stable configuration of the cyclohexane-oxygen complex is presented in Fig. 3. Earlier calculations of the structure for this complex have been carried out by Parsons and Chandler[28] with the use of B3LYP/6-31g(d) approach. These authors found the so-called "resting" structure [Fig. 1(b) of Ref. 28] to be the most stable one. In that geometry the center of electron density is located perfectly in the T-position with respect to O_2 molecule. It is now recognized that the dispersion interaction affecting the equilibrium geometry and binding energy of weakly bound complexes cannot be reproduced within the standard version of DFT theory and particularly within the DFT-BLYP approach.[29] Use of the more adequate MP2 approach can shift global minimum for geometry of the complex as compared with the DFT result and is more appropriate for the calculation of binding energy. When we calculated the resting structure as a starting one, we found that optimization within MP2/6-31++G(d,p) approach with BSSE correction provided a new

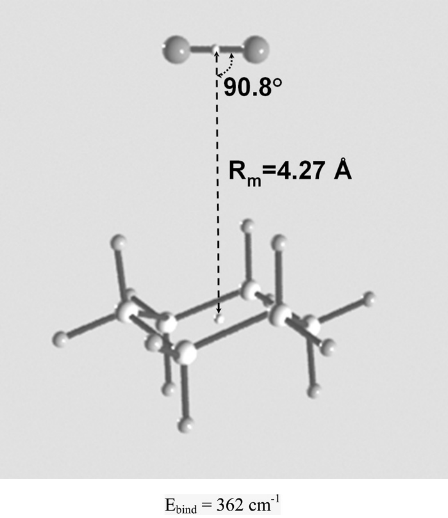

FIG. 3. The most stable configuration of the van der Waals complex C_6H_{12}—O_2 (C_S symmetry) and its binding energy obtained by *ab initio* calculations using approach 2 as described in the text. The symmetry plane includes the oxygen molecule and the diagonal of the cyclohexane ring. The line connects the center of the O_2 molecule with the center of mass of cyclohexane, shown by point.

minimum with the structure shown in Fig. 3, and a calculated binding energy of 362 cm^{-1}. This new minimum corresponds to a structure with C_S symmetry and very small (0.06 Å) displacement of the center of the O_2 molecule from the point against the center of mass of cyclohexane. Figure 3 also shows that the direction from the center of mass of C_6H_{12} to the center of O_2 molecule is almost perpendicular to the O—O bond. We can thus conclude that the most stable structure of C_6H_{12}—O_2 complex is very close to the T-shaped one. Attempts to use different configurations as starting points provided after optimization a less strongly bound complex structure.

D. C_3H_6—O_2

The most stable configuration of the propylene-oxygen complex is presented in Fig. 4. The configuration of oxygen is found to be near T-shaped relative to the center of the CC double bond of propylene. The value of the binding energy calculated using approach 2 is presented in the figure as well.

V. EXPERIMENTAL RESULTS

The full set of data is presented in Ref. 15. Here we represent only the central part of the sliced images for all clusters and for individual O_2 molecules (Fig. 5). Channel 1, which is the subject of interest in the present paper, is indicated by arrows. This channel corresponds to the prompt dissociation of clusters into the products X, O, and O, where the ring corresponding to channel 1 in the O(^3P_j) atom image is smaller in size than the ring originating from the dissociation of free O_2 molecules.[15] Also, for all clusters studied, channel 1 has a negative anisotropy that means that O atoms fly more or less preferentially perpendicular to the direction of linear polarization of the laser radiation. Figure 5 demonstrates this for all the complexes besides Xe—O_2. The image for Xe—O_2 contains a visible contribution from O atoms resulting from photodissociation of unbound O_2, which provides a rather parallel image, Fig. 5(a). While this contribution masks the negative anisotropy of the O atoms arising from X–O_2 in Fig. 5(b), after subtraction of the image due to dissociation of unbound O_2, as described in the experimental section, a slightly negative anisotropy is revealed for this complex as well. The quantitative values of kinetic energy of O atoms corresponding to the maximum of the intensity of the ring and the value of anisotropy parameter β for channel 1 for all studied clusters are represented in Table I.

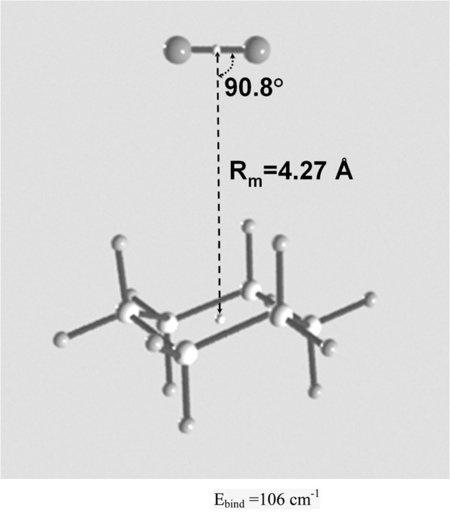

FIG. 4. The binding energy and most stable configuration of the van der Waals cluster C_3H_6—O_2 obtained by *ab initio* calculations using approach 2 described in the text. The line shown connects the center of the O_2 molecule with the center of the CC double bond.

VI. DISCUSSION

The fragment kinetic and internal energy for photodissociation of the X–O_2 cluster into X, O, and O fragments must

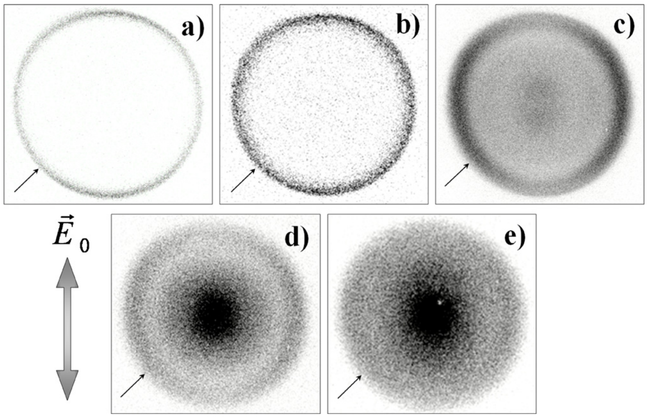

FIG. 5. Sliced images (Ref. 15) of O($^3P_2$) atoms arising from the photodissociation of individual O_2 molecules and X–O_2 clusters at the wavelength of 225.655 nm ((2+1) REMPI of O($^3P_2$) atoms). (a) Pure O_2; (b) Xe—O_2 clusters; (c) CH_3I—O_2 clusters; (d) C_6H_{12}—O_2 clusters; and (e) C_3H_6—O_2 clusters. For all images only the central part, corresponding to the kinetic energy of O atoms less than 2000 cm^{-1} is shown. The arrows on the images (b)–(e) indicate channel 1 (see test for details). The arrow on the image (a) indicates the ring corresponding to the process (1) that was used for kinetic energy calibration. The direction of polarization of the excitation laser is indicated by double-headed arrow.

TABLE I. Experimental values of kinetic energy, angular anisotropy, and van der Waals binding energy for oxygen atoms arising in channel 1 from different X–O_2 complexes.

Complex	T_1 (cm^{-1})	β	D_{vdW} (cm^{-1})
Xe—O_2	1352 ± 8	-0.20 ± 0.02	110 ± 20
CH_3I—O_2	1298 ± 8	-0.48 ± 0.02	280 ± 20
C_6H_{12}—O_2	1087 ± 8	-0.17 ± 0.02	585 ± 20
C_3H_6—O_2	1166 ± 8	-0.31 ± 0.02	135 ± 30

be in agreement with the energy conservation law. With the assumption of an originally unexcited X–O_2 complex we can write

$$h\nu = D_{vdW}(X - O_2) + D_0(O_2) + T_{O1} + T_{O2} + E_{int\ 1} + E_{int\ 2} + T_X + E_{int\ X}. \tag{3}$$

In this equation $h\nu = 44\,315.5\ cm^{-1}$, $D_0(O_2) = 41\,268.6 \pm 1.1\ cm^{-1}$ (Ref. 26) is the energy of O_2 dissociation giving rise to two ground state $O(^3P_2)$ atoms, $D_{vdW}(X-O_2)$—is the energy of van der Waals bond X–O_2, T_{O1}, and $E_{int\ 1}$—the kinetic and internal energy of the oxygen atom that we ionize and observe, T_{O2} and $E_{int\ 2}$—the kinetic and the internal energy of another oxygen atom, and T_X and $E_{int\ X}$—the kinetic and the internal energy of the fragment X.

In order to determine the van der Waals bond energy, one needs to know the kinetic energy and internal energy of all three (X, O, and O) fragments. $E_{int\ 1}=0$ since we observe O^+ ions produced as a result of the selective ionization of $O(^3P_2)$. Since the other O atom can be produced in the $^3P_2$, $^3P_1$, and $^3P_0$ states, we assume the branching ratio to be the same as in the calibration experiment and equal to that measured for photodissociation of O_2 at 226 nm,[27] since DeBoer and Young[30] have shown that the branching ratio for the $O(^3P_j)$ fine states arising in the photodissociation of the X–O_2 (X=C_6H_6) van der Waals complex is the same as that for photodissociation of O_2 at 226 nm. Using this assumption, we substitute the term $E_{int\ 2}$ in Eq. (3) with the average value $\langle E_{int\ 2}\rangle = (0.66 \cdot 0 + 0.27 \cdot 158.265 + 0.07 \cdot 226.977) = 58.6\ cm^{-1}$. Note that the term $\langle E_{int\ 2}\rangle$ is equal to the term $\langle E_{int}(^3P_J)\rangle_0$ introduced earlier in discussion of calibration experiment, since we assume the same branching ratio both in the calibration experiment and in the experiments with clusters.

After these simplifications we still have the T_{O2}, T_X, and $E_{int\ X}$ terms in Eq. (3), which are not measured in our experiment. In the following text, we show how we can determine those terms with the use of experimentally measured kinetic energy and angular anisotropy of the $O(^3P_2)$ atoms. In order to do this we use the following data:

(1) We know the geometry of the X–O_2 cluster ground state is T-shaped or close to T-shaped, where the center of the X partner is located in or near the T-position relative to O_2 molecule.

(2) For the T-shaped Xe—O_2 or the nearly T-shaped CH_3I—O_2 and C_6H_{12}—O_2 complexes the transition dipole moment has been concluded to be directed along the X–O_2 axis of the complex.[15]

(3) The kinetic energy has to be shared between the products X, O, and O in accord with momentum conservation.

(4) For O atoms, we know the value of the anisotropy parameter describing the angular distribution of their recoil directions.

Below, we will show how the combination of these data can be used in the case of an ideal T-shaped cluster, where X partner is a point mass perfectly located in the T-position. After that, we will adapt the obtained conclusions and equations to the actual X partners used in our study.

A. Photodissociation of a T-shaped cluster with X as a point-mass particle

Since the complex is perfectly T-shaped, we assume that before and during the entire recoil process both O atoms move symmetrically with respect to the axis passing through X and the center of O—O bond. Thus, $T_{O1} = T_{O2} = T_1$. When using this and the above-mentioned equality $\langle E_{int\ 1}\rangle = 0$, we can rewrite Eq. (3) as

$$h\nu = D_{vdW}(X - O_2) + D_0(O_2) + 2 \cdot T_1 + \langle E_{int\ 2}\rangle + T_X + E_{int\ X}, \tag{4}$$

and express the van der Waals bond energy

$$D_{vdW}(X - O_2) = h\nu - D_0(O_2) - \langle E_{int\ 2}\rangle - 2 \cdot T_1 - T_X - E_{int\ X}. \tag{5}$$

For the case of free O_2 photodissociation with $D_{vdW}(X-O_2)$, T_X and $E_{int\ X}$ equal to zero, this equation gives

$$h\nu - D_0(O_2) - \langle E_{int2}\rangle = 2 \cdot T_0, \tag{6}$$

where T_0 is the kinetic energy of the oxygen atoms arising from free O_2. As discussed above, we can assume the equality of $\langle E_{int\ 2}\rangle$ values in Eqs. (5) and (6) for photodissociation of complexed and free O_2, respectively. Rewriting Eq. (5) as

$$D_{vdW}(X - O_2) = 2 \cdot T_0 - 2 \cdot T_1 - T_X - E_{int\ X}. \tag{7}$$

Figure 6 describes the geometry of the photodissociation of an ideal T-shaped X–O_2 cluster with a point-mass X. The coordinate system on that figure is introduced in such a way that the plane $y'z'$ coincides with the plane of cluster. The y' axis goes through both oxygen atoms, and axis z' goes through the center of the particle X and the middle of O—O bond. The transition dipole moment for the transition giving rise to channel 1 is shown to be directed along the X–O_2 (z') axis of the complex as was earlier concluded in Ref. 15 on the basis of the analysis of experimental images.

The velocities of the fragments arising in the dissociation are denoted as $\vec{v}_X$, $\vec{v}_{O_1}$, and $\vec{v}_{O_2}$. We assume conservation of C_{2V} symmetry during the dissociation of cluster. This means particularly, that the vectors $\vec{v}_{O_1}$ and $\vec{v}_{O_2}$ have the same absolute values (later on, we will denote this value as v_1) and the same angle γ between the velocity vector and the z' axis (Fig. 6). Conservation of the projection of the total momentum of the cluster on z' axis gives the equation

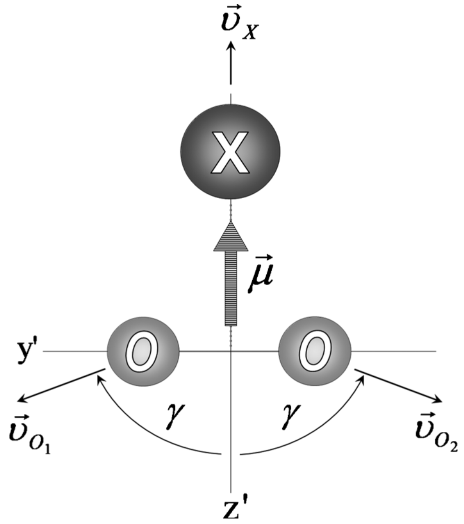

FIG. 6. Dissociation geometry of an ideal T-shaped $X-O_2$ complex following the photoexcitation with the transition dipole moment parallel to $C_2(z')$ axis of the complex. Coordinate axis y′ goes through two O atoms; axis z′ goes through particle X and through the middle of the O—O bond. The striped arrow indicates the transition dipole moment vector $\vec{\mu}$, which is directed toward X and lies parallel with the z′ axis. Vectors $\vec{\upsilon}_X$, $\vec{\upsilon}_{O_1}$, and $\vec{\upsilon}_{O_2}$ indicate the velocities of the fragment X and two oxygen atoms after the dissociation. Symmetry is conserved during the entire dissociation process, which means that particle X is always moving along the axis z′, and that both oxygen atoms are always symmetrically moving with respect to the axis z′. The angles between the final directions of velocities $\vec{\upsilon}_{O_1}$ and $\vec{\upsilon}_{O_2}$ and axis z′ are indicated as γ.

$$2 \cdot m_O \cdot \upsilon_1 \cdot \cos \gamma = m_X \cdot \upsilon_X, \tag{8}$$

where m_O and m_X are the masses of oxygen atom and of particle X, respectively. From Fig. 6 one can see that the angle γ is actually the angle between the recoil direction of O atoms and the direction of the transition dipole moment $\vec{\mu}$. This angle has a well-known experimental meaning; in the general case of one quantum photodissociation induced by linearly polarized light the fragments recoil angular distribution is described by[31]

$$\frac{dN}{d\Omega} \propto \left(1 + \beta \cdot \left(\frac{3}{2}\cos^2 \theta - \frac{1}{2}\right)\right), \tag{9}$$

where β is the anisotropy parameter, which can be experimentally measured by fitting the experimental angular distribution by Eq. (9). The value of β is related to the geometry of recoil by the expression[31]

$$\beta = (3 \cos^2 \gamma - 1). \tag{10}$$

If now we express $\cos^2 \gamma$ from Eq. (10), substitute it into Eq. (8) and convert the speed to kinetic energy, we then obtain the following expression:

$$T_X = 2 \cdot T_1 \cdot \left(\frac{2}{3}(\beta + 1)\frac{m_0}{m_X}\right). \tag{11}$$

Using this expression, we can modify Eq. (7) and finally obtain

$$D_{vdW}(X - O_2) = 2 \cdot T_0 - 2 \cdot T_1 - 2T_1 \cdot \left(\frac{2}{3}(\beta + 1)\frac{m_0}{m_X}\right) - E_{int\,X}. \tag{12}$$

The right side of this formula contains the known values m_O and m_X and the characteristics T_0, T_1, and β for oxygen atoms from channel 1, which are measured in the experiment. The only uncertain value is internal energy $E_{int\,X}$ of the fragment X produced by the photodissociation. Since the state of X is not changed during the excitation process the internal energy of this molecule should not change in the process of photoexcitation. Later, when we consider the application of Eq. (12) to real $X-O_2$ complexes, we will discuss the possibility that this term is nonzero.

The equations allow us to make conclusions on the possible range of variation of the angular anisotropy parameter. This variation is governed by the degree of partitioning the total kinetic energy T_{tot} of the photofragments O_1, O_2, and X into "parallel," $T_\parallel$, and "perpendicular," $T_\perp$ parts. $T_\parallel$ corresponds to the kinetic energy of translation along the z′ axis, and $T_\perp$ corresponds to the kinetic energy of translation along y′ axis, which is perpendicular to the direction of transition dipole moment of the complex. For decay of the T-shaped complex shown in Fig. 6 the angular anisotropy parameter β is equal to −1 when the projection of the velocities $\vec{\upsilon}_{O_1}$ and $\vec{\upsilon}_{O_2}$ on the z′ axis are equal to 0 and so the angle $\gamma=0$. In this case $T_\parallel=0$ and the total kinetic energy T_{tot} of the photofragments is equal to $T_\perp$. In the general case the total kinetic energy of the photofragments is equal to $T_{tot}=T_\parallel+T_\perp=T_X+T_{O1}+T_{O2}=T_X+2T_1$. The parallel part of kinetic energy is equal to

$$T_\parallel = T_X + 2T_1 \times \cos^2 \gamma = 2T_1 \cdot \frac{(1+\beta)}{3} \cdot \left(\frac{m_X + 2m_O}{m_X}\right), \tag{13}$$

and the perpendicular part is equal to

$$T_\perp = T_{tot} - T_\parallel = T_X + 2T_1 - T_\parallel = 2T_1 \cdot \left(1 - \frac{(1+\beta)}{3}\right). \tag{14}$$

The contributions of $T_\parallel$ and $T_\perp$ are governed by the shape of the potential energy surface for the $X-O_2$ complex in the excited electronic state that gives rise to channel 1. In the excited state, the minimum of the van der Waals potential is expected to be shifted to a longer $X-O_2$ distance as compared with the ground state. "Vertical" excitation should thus deliver the complex to the wall of the potential in the excited state with nonzero force providing repulsion in the $X-O_2$ pair, with the resulting nonzero value of $T_\parallel$. According to Eqs. (13) and (14), the variation of $T_\parallel$ within the range from 0 to T_{tot} provides variation of the angular anisotropy parameter β from −1 to 2. Even for an ideal T-shaped complex with photodissociation shown in the scheme of Fig. 6, the image of O atoms can be perpendicular or parallel depending on the shape of PES in the excited state of complex.

B. $Xe—O_2$

According to the experimental results reported by Aquilanti *et al.*[13] and results of calculations reported in the present paper (Fig. 1), the global minimum of the van der Waals potential energy surface for $Xe—O_2$ corresponds to the T-shaped configuration. In both of the studies the linear structure for $Xe—O_2$ was found to be less stable than the T-shaped one, and so we believe that in the supersonic expansion in our experiments the dominant part of $Xe—O_2$ clusters are T-shaped. Therefore, these complexes perfectly match the ideal case considered in Sec. V and can be described by formula (12). In order to determine the value of the van der Waals bond energy, we have to substitute the values for the detected oxygen isotope ^{16}O mass $m_O = 15.995$ amu,[32] and the atomic weight of xenon averaged over its isotopic composition $m_X = m_{Xe} = 131.293$ amu,[32] and the values of β and T_1 from Table I ($\beta = -0.20 \pm 0.02$, and $T_1 = 1343 \pm 8$ cm^{-1}). Since the first excited level of Xe lies very high in energy [67 067.547 cm^{-1} (Ref. 23)] and cannot be accessed in this process, we set $E_{int\,X} = E_{int\,Xe} = 0$ in formula (12). After the calculation, we obtain the value of van der Waals binding energy for $Xe—O_2$ to be $D_{vdW}(Xe—O_2) = 110 \pm 20$ cm^{-1}. The uncertainty presented is governed by the experimental uncertainties of β and the T_1 values.

This value can be compared with the other data for the binding energy of the $Xe—O_2$ complex (Fig. 1). Aquilanti *et al.*[13] reported a value of 144 ± 7 cm^{-1} for the T-shaped geometry. Their value was obtained in experiments on scattering aligned O_2 molecules with Xe atoms. Our experimental result of 110 ± 20 cm^{-1} is slightly lower than that by Aquilanti.[13] Taking into account the experimental uncertainty of both results we can conclude that these two values are suitably close. The binding energy calculated for the T-shaped geometry of this complex (see Fig. 2) using the more sophisticated approach 2 is equal to 86 cm^{-1}, which slightly underestimates the experimental result.

C. $CH_3I—O_2$

According to our *ab initio* calculations represented in Fig. 2, $CH_3I—O_2$ clusters have several stable configurations with close binding energy values. In the configuration with $\theta \approx 180°$, the iodine atom is the closest to O_2 molecule, and in the other two the position of the C-atom is closer to O_2 by 0.3 Å as compared with that of the I-atom. Taking into account the size of the I-atom we can assume that during the dissociation the O atoms mainly “feel” the iodine atom. In all three configurations, the I-atom is located close to the T-position with respect to the O_2 molecule. Subsequently, as in the impulsive model suggested earlier by Busch and Wilson,[33] we can assume that the energy released is shared by the O atoms and the iodine atom in accord with conservation of momentum. Since the iodine atom is also donor of the electron in the charge-transfer state of this cluster, the direction of transition dipole moment should be directed from the I atom to the O_2 molecule. We can consider dissociation of the $CH_3I—O_2$ complex to correspond with the dissociation scheme shown in Fig. 6 with the iodine atom as partner X. This means that for $CH_3I—O_2$ we can use formula (12) assuming $m_X = m_I = 126.9$ amu., and values of β and T_1 from the Table I ($\beta = -0.48 \pm 0.02$, and $T_1 = 1290 \pm 8$ cm^{-1}). Electronic excitation of the CH_3I subunit cannot accompany the photodissociation of O_2 in the complex because the total excited energy is too high. Therefore, we can set $E_{int\,X} = 0$ in formula (12). After calculation we obtain 280 ± 20 cm^{-1} for the van der Waals binding energy of $CH_3I—O_2$. The binding energy calculated for the most stable configuration of this complex (see Fig. 2) following approach 2 is equal to 203 cm^{-1}, which underestimates the experimental result.

D. $C_6H_{12}—O_2$

The structure of the most stable configuration of the $C_6H_{12}—O_2$ complex is very close to T-shaped, as shown in Fig. 3. The C_6H_{12} molecule has no distinctive localized center with a large polarizability such as iodine in CH_3I. As discussed above, the photoexcitation of the complex appears to place the molecule on the wall of the excited state potential $C_6H_{12}—O_2{}^*$ where O_2 is excited to the Herzberg III ($^3\Delta_u$) state. For the structure shown in Fig. 3, we can expect that during the dissociation process the repelling forces are symmetric and the resultant force is applied close to the center of cyclohexane, giving no vibrational or rotational excitation to the cyclohexane frame. Therefore for $C_6H_{12}—O_2$ clusters we can use formula (12) with $E_{int\,X} = 0$, $m_X = m_{C6H12} = 84$ amu, and the values of β and T_1 from the Table I ($\beta = -0.17 \pm 0.02$ and $T_1 = 1080 \pm 8$ cm^{-1}). After calculation we obtain 585 ± 20 cm^{-1} for the $C_6H_{12}—O_2$ van der Waals bond energy.

We could not find any data on the $C_6H_{12}—O_2$ van der Waals binding energy in the literature. A comparison can be made with the experimental data of Grover *et al.*[5] who measured the value of $C_6H_6—O_2$ van der Waals binding energy in clusters by measuring of the threshold of appearance of $C_6H_6{}^+$ product in the excitation of $C_6H_6—O_2$ by tunable synchrotron radiation. We believe that the van der Waals bond energy in $C_6H_{12}—O_2$ and $C_6H_6—O_2$ should be quite similar. In the absence of permanent dipole moments in any of these partners, the intermolecular interaction energy is governed by the dispersive interaction that, in turn, is determined by the polarizability of the complex partners and by the number of electrons in the highest quantum numbers.[34] These last numbers are the same as well as polarizability values are similar for molecules C_6H_{12} and C_6H_6 as presented in the Ref. 35. All of this allows us to expect a similarity in binding energy values for these complexes. Our determined value of the binding energy for $C_6H_{12}—O_2$ of 585 ± 20 cm^{-1} is in perfect agreement with the value of 1.6 ± 0.3 kcal/mol (560 ± 105 cm^{-1}) measured for the $C_6H_6—O_2$ complex by Grover *et al.*[4] The binding energy calculated for the most stable configuration of this complex (see Fig. 3) using approach 2 is equal to 362 cm^{-1}, which again underestimates the experimental result.

E. $C_3H_6—O_2$

For the extraction of the value for van der Waals binding energy for the $C_3H_6—O_2$ complex, we used formula (12) and several assumptions.

1. We assume that the transition dipole moment is directed from the middle of the O—O bond to the middle of the C=C double bond, because in the charge transfer state of this complex the electron is transferred from the double bond orbital of propylene. This vector is almost perpendicular to the O—O bond (92.8° according to the calculated structure shown in Fig. 4). We will assume it to be perfectly perpendicular in order to maintain recoil symmetry between the two O atoms.
2. The total loss of energy transferred to the O atoms as compared with photodissociation of the free O_2 molecule is only about $2\times\Delta T=2\times T_0-2\times T_1 \approx 650\ \text{cm}^{-1}$ which is less than any vibrational energy in the C_3H_6 molecule. A vibrational contribution to $E_{\text{int X}}$ can thus be neglected as well as any electronic contribution.
3. To consider the contribution of rotational energy we treat C_3H_6 as a rigid molecule during the dissociation process. We assume that C_3H_6 obtains translational momentum and angular momentum (rotational excitation) by an instant kick directed from the center of the O=O molecule to the center of the C=C double bond. In this kick, the momentum P_X is imparted to the middle of the C=C bond. We also consider C_3H_6 as a rigid classical frame. Since the recoil axis does not pass through the center of mass of the C_3H_6 molecule it will cause some rotation.

We assume C_3H_6 to behave as a rigid classical frame and give the expression for the value of rotational energy obtained by C_3H_6

$$E_{\text{rot X}} = \frac{P_X^2 \cdot L^2}{2 \cdot I_X}, \tag{15}$$

where $L=0.649$ Å—is the arm of the momentum $\vec{P}_X$ relative to the center of mass of the C_3H_6 molecule, and $I_X = 63.4$ amu Å^2—the momentum of inertia of C_3H_6 molecule with respect to the center of mass. The values of L and I_X are calculated based on the structure of $C_3H_6—O_2$ shown in Fig. 4. Substituting this expression instead of $E_{\text{int X}}$ into formula (12) and considering the fact that translational momentum of propylene P_X can be expressed via T_1 using Eqs. (8) and (13) we finally obtain for the $C_3H_6—O_2$ van der Waals binding energy

$$D_{\text{vdW}}(X-O_2) = 2\cdot T_0 - 2\cdot T_1 - 2T_1\cdot\left(\frac{2}{3}(\beta+1)\frac{m_0}{m_X}\right)\cdot\left(1+\frac{L^2\cdot m_X}{I_X}\right). \tag{16}$$

We set the values of $m_X=m_{C3H6}=42.1$ amu,[24] $\beta=-0.31\pm0.02$, and $T_1=1158\pm8\ \text{cm}^{-1}$ from Table I, and the above-mentioned values of L and I_X. After calculation we obtain $135\pm30\ \text{cm}^{-1}$ for the $C_3H_6—O_2$ van der Waals bond. The binding energy calculated for the most stable configuration of this complex (see Fig. 4) following approach 2 is equal to $106\ \text{cm}^{-1}$, which slightly underestimates the experimental result.

VII. FURTHER REMARKS

Our method is a modification of previously existing methods based on measurement of the kinetic energy of photodissociation products, and calculation of the energy of the broken bond using the energy conservation law. The invention of velocity map imaging[24] has made this method especially powerful. We can refer to the studies of Eppink *et al.*,[36] Nahler *et al.*,[37] and Chestakov *et al.*[38] where the energy of C—I bond in CH_3I molecule, the dissociation energy of $BrCl^+$ ion and FeO molecule were measured, respectively. In the usual applications of this method the studied molecule or ion dissociates into two fragments. The kinetic energy is measured for one of the fragments, and for the other fragment the kinetic energy is calculated using momentum conservation.

In the present study the $X-O_2$ van der Waals clusters dissociate into three fragments and therefore the relation between the kinetic energy of the fragment X and the kinetic energy of the O atoms is not as trivial as in the case of two fragments. Some knowledge is assumed about the cluster geometry, the direction of transition dipole moment and the experimentally measured value of the anisotropy parameter for recoil of the O atoms.

The validity of our method can be checked by comparison of the van der Waals bond energy obtained by the described method and values independently determined. Such a comparison is possible for the $Xe—O_2$ complex and shows reasonable agreement with the present approach and previously obtained data from scattering experiments. In the development of the method we did not use any specific properties of oxygen molecule. It means that in principal this method can be applied to any $X-Y_2$ type T-shaped clusters.

VIII. CONCLUSIONS

In this paper, a new approach for the experimental determination of the binding energy of van der Waals complexes as well as the results of its application for the $X-O_2$ complexes ($X=Xe$, CH_3I, C_3H_6, and C_6H_{12}) is described. This approach is based on the determination of the kinetic energies of the X, O, and O products arising in the photodissociation of $X-O_2$, and the calculation of the van der Waals bond energy based on energy conservation. This analysis was applied to the channel for prompt dissociation of $X-O_2$ into X, O, and O, which is observed for complexes of O_2 with any molecule X. As was earlier concluded[15] the direction of this transition dipole moment for the complexes under study is perpendicular to the O—O bond. In the approach used, the kinetic energy of O atoms is directly measured. The kinetic energy of the X fragment is calculated with the use of momentum conservation and the values of the measured kinetic energy and angular anisotropy of O atoms. An unambiguous relation between the kinetic energy of the X molecule and the O atoms becomes possible for T-shaped complexes. To check this for the Xe—O_2, CH_3I—O_2, C_6H_{12}—O_2, and C_3H_6—O_2 clusters *ab initio* calculations of the structure and energy were performed. The structure of the most stable configuration was found to be T-shaped or very close to that for the Xe—O_2, CH_3I—O_2, and C_6H_{12}—O_2 complexes. Binding energy values are then determined to be $110 \pm 20\ \text{cm}^{-1}$, $280 \pm 20\ \text{cm}^{-1}$, and $585 \pm 20\ \text{cm}^{-1}$, respectively. In the most stable configuration of the C_3H_6—O_2 complex, the double bond of C_3H_6 was found to be located in the T-position with respect to the O_2 molecule, which has also allowed us to estimate the binding energy to be $135 \pm 30\ \text{cm}^{-1}$.

The T-shaped geometry is expected to prevail for complexes X–O_2 with symmetric X subunits. The suggested approach of van der Waals binding energy determination can be also applied for other complexes of the type X–Y_2.

ACKNOWLEDGMENTS

We gratefully acknowledge financial support from the Netherlands Organization for Scientific Research (NWO) under the programs Molecular Atmospheric Physics (MAP-09), NWO-CW ECHO Project No. 700.55.025, and NWO Russia-Netherlands Cooperative Research Grant No. 047.009.001 as well as the financial support of this work by Russian Foundation for Basic Research (Grant No. 09-03-00310-a).

[1] Chem. Rev. (Washington, D.C.) 88, entire issue (1988).

[2] Chem. Rev. (Washington, D.C.) 94, entire issue (1994).

[3] Chem. Rev. (Washington, D.C.) 100, entire issue (2000).

[4] W. B. Schweizer and J. D. Dunitz, J. Chem. Theory Comput. **2**, 288 (2006).

[5] J. R. Grover, G. Hagenow, and E. A. Walters, J. Chem. Phys. **97**, 628 (1992).

[6] H. Krause, B. Ernstberger, and H. J. Neusser, Chem. Phys. Lett. **184**, 411 (1991).

[7] B.-M. Cheng, J. R. Grover, and E. A. Walters, Chem. Phys. Lett. **232**, 364 (1995).

[8] A. Courty, M. Mons, I. Dimicoli, F. Piuzzi, M.-P. Gaigeot, V. Brenner, P. de Rujo, and P. Millie, J. Phys. Chem. A **102**, 6590 (1998).

[9] J. E. Braun, T. Mehnert, and H. J. Neusser, Int. J. Mass Spectrom. **203**, 1 (2000).

[10] J. P. Darr, J. J. Glennon, and R. A. Loomis, J. Chem. Phys. **122**, 131101 (2005).

[11] A. Burroughs and M. C. Heaven, J. Chem. Phys. **114**, 7027 (2001).

[12] J. A. Blazy, B. M. DeKoven, T. D. Russell, and D. H. Levy, J. Chem. Phys. **72**, 2439 (1980).

[13] V. Aquilanti, D. Ascenzi, D. Cappelletti, M. Castro, and F. Pirani, J. Chem. Phys. **109**, 3898 (1998).

[14] D. Cappelletti, M. Bartolomei, E. Carmona-Novillo, F. Pirani, G. Blanquet, and F. Thibault, J. Chem. Phys. **126**, 064311 (2007).

[15] A. V. Baklanov, G. A. Bogdanchikov, K. V. Vidma, D. A. Chestakov, and D. H. Parker, J. Chem. Phys. **126**, 124316 (2007).

[16] S. F. Boys and F. Bernardi, Mol. Phys. **19**, 553 (1970).

[17] T. N. Dunning, Jr., J. Chem. Phys. **90**, 1007 (1989).

[18] J. M. L. Martin and A. Sunderman, J. Chem. Phys. **114**, 3408 (2001).

[19] A. Bergner, M. Dolg, W. Kuechle, H. Stoll, and H. Preuss, Mol. Phys. **80**, 1431 (1993).

[20] EMSL Basis Set Library, http://www.emsl.pnl.gov:2080/forms/basisform.html/.

[21] K. A. Peterson, D. Figgen, E. Goll, H. Stoll, and M. Dolg, J. Chem. Phys. **119**, 11113 (2003).

[22] M. J. Frisch, G. W. Trucks, H. B. Schlegel *et al.*, GAUSSIAN 03, Revision C.02, Gaussian, Inc., Wallingford, CT, 2004.

[23] Yu. Ralchenko, A. E. Kramida, J. Reader, and NIST ASD Team, NIST Atomic Spectra Database (version 3.1.5), [Online]. Available: http://physics.nist.gov/asd3. National Institute of Standards and Technology, Gaithersburg, MD (2008).

[24] A. T. J. B. Eppink and D. H. Parker, Rev. Sci. Instrum. **68**, 3477 (1997).

[25] D. Chestakov, S.-M. Wu, G. Wu, D. H. Parker, A. T. J. B. Eppink, and T. N. Kitsopoulos, J. Phys. Chem. A **108**, 8100 (2004).

[26] P. C. Cosby and D. L. Huestis, J. Chem. Phys. **97**, 6108 (1992).

[27] K. Tonokura, N. Shafer, Y. Matsumi, and M. Kawasaki, J. Chem. Phys. **95**, 3394 (1991).

[28] B. F. Parsons and D. W. Chandler, J. Phys. Chem. A **107**, 10544 (2003).

[29] S. Grimme, J. Comput. Chem. **25**, 1463 (2004).

[30] G. DeBoer and M. A. Young, J. Chem. Phys. **106**, 5468 (1997).

[31] R. N. Zare, *Angular momentum, Understanding Spatial Aspects in Chemistry and Physics* (John Wiley and Sons, Inc., New York, 1988).

[32] http://physics.nist.gov/PhysRefData/Compositions/index.html On-line database, developed by NIST (J. S. Coursey, D. J. Schwab, and R. A. Dragoset NIST, Physics Laboratory, Office of Electronic Commerce in Scientific and Engineering Data).

[33] G. E. Busch and K. R. Wilson, J. Chem. Phys. **56**, 3626 (1972).

[34] J. C. Slater and J. G. Kirkwood, Phys. Rev. **37**, 682 (1931).

[35] *CRC Handbook of Chemistry and Physics*, 77th ed., edited by D. R. Lide (CRC, Boca Raton, FL, 1996).

[36] A. T. J. B. Eppink and D. H. Parker, J. Chem. Phys. **109**, 4758 (1998).

[37] N. H. Nahler, O. P. J. Vieuxmaire, J. R. Jones, M. N. R. Ashfold, A. T. J. B. Eppink, A. M. Coriou, and D. H. Parker, J. Phys. Chem. A **108**, 8077 (2004).

[38] D. A. Chestakov, D. H. Parker, and A. V. Baklanov, J. Chem. Phys. **122**, 084302 (2005).